Discovery of Ultra-Compact Dwarf Galaxies in the Virgo Cluster

J. B. Jones
Astronomy Unit, School of Mathematical Sciences, Queen Mary University of London, Mile End Road, London, E1 4NS, U.K.

M. J. Drinkwater and R. Jurek
Department of Physics, University of Queensland, Queensland 4072, Australia

S. Phillipps
Astrophysics Group, Department of Physics, University of Bristol, Tyndall Avenue, Bristol, BS8 1TL, U.K.

M. D. Gregg[1]
Department of Physics, University of California, Davis, CA 95616, U.S.A.

K. Bekki and W. J. Couch
School of Physics, University of New South Wales, Sydney 2052, Australia

A. Karick
Institute for Geophysics and Planetary Physics, Lawrence Livermore National Laboratory, L-413, Livermore, CA 94550, U.S.A.

Q. A. Parker[2]
Department of Physics, Macquarie University, Sydney, New South Wales 2109, Australia
and

R. M. Smith
School of Physics and Astronomy, University of Wales Cardiff, P.O. Box 913, Cardiff, CF12 3YB, U.K.

ABSTRACT

We have discovered nine ultra-compact dwarf galaxies (UCDs) in the Virgo Cluster, extending samples of these objects outside the Fornax Cluster. Using the 2dF multi-fiber spectrograph on the Anglo-Australian Telescope, the new Virgo members were found among 1500 color-selected, star-like targets with $16.0 < b_j < 20.2$ in a two-degree diameter field centered on M87 (NGC4486).

[1]Institute for Geophysics and Planetary Physics, Lawrence Livermore National Laboratory, L-413, Livermore, CA 94550, U.S.A.

[2]Anglo-Australian Observatory, P. O. Box 296, Epping, NSW 1710, Australia.

The newly-found UCDs are comparable to the UCDs in the Fornax Cluster, with sizes $\lesssim 100$ pc, $-12.9 < M_B < -10.7$, and exhibiting red, absorption-line spectra, indicative of an older stellar population. The properties of these objects remain consistent with the tidal threshing model for the origin of UCDs from the surviving nuclei of nucleated dwarf ellipticals disrupted in the cluster core, but can also be explained as objects that were formed by mergers of star clusters created in galaxy interactions. The discovery that UCDs exist in Virgo shows that this galaxy type is probably a ubiquitous phenomenon in clusters of galaxies; coupled with their possible origin by tidal threshing, the UCD population is a potential indicator and probe of the formation history of a given cluster.

We also describe one additional bright UCD with $M_B = -12.0$ in the core of the Fornax Cluster. We find no further UCDs in our Fornax Cluster Spectroscopic Survey down to $b_j = 19.5$ in two additional 2dF fields extending as far as 3° from the center of the cluster. All six Fornax bright UCDs identified with 2dF lie within 0.°5 (projected distance of 170 kpc) of the central elliptical galaxy NGC1399.

Subject headings: galaxies: clusters: individual (Virgo, Fornax) — galaxies: dwarf — galaxies: distances and redshifts — galaxies: peculiar — surveys

1. Introduction

Compact dwarf galaxies are an established constituent of the population of lower luminosity galaxies, alongside the more numerous dwarf irregular, dwarf elliptical and dwarf spheroidal galaxies. Of compact dwarfs, early-type compact ellipticals like M32, showing early-type galaxy spectra, are rare and only very few examples have been found (Faber 1973, Nieto & Prugniel 1987). Blue compact dwarfs show active star formation superimposed on an older low surface brightness component, and have a broad range in sizes, including a very small proportion with effective radii as small as 300 pc (e.g. Doublier, Caulet & Comte 1999; Cairós et al. 2001; Gil de Paz, Madore & Pevunova 2003). The extremely compact star-forming object POX186 has been described by, among others, Kunth et al. (1988), Doublier et al. (2000) and Corbin & Vacca (2002).

However, a new class of compact galaxy, more than an order of magnitude smaller in physical size than conventional compact dwarfs, has recently been discovered in the Fornax Cluster. Hilker et al. (1999) found two very compact objects in a spectroscopic survey of the cluster with a fiber-fed spectrograph on the 2.5-metre du Pont Telescope. Meanwhile, Drinkwater et al. (2000a; see also Phillipps et al. 2001; Drinkwater et al. 2002) identified five objects that had velocities of cluster galaxies and which were either unresolved or marginally resolved in ground-based imaging during the Fornax Cluster Spectroscopic Survey (FCSS; Drinkwater et al. 2000b), including the two Hilker et al. objects. The five compact objects had blue absolute magnitudes $-13 \leq M_B \leq -11$, and sizes $\ll 100$ pc: they were therefore named "ultra-compact dwarfs" (UCDs).

Possible explanations for these ultra-compact dwarfs include unusually luminous globular clusters (e.g. Hilker et al. 1999; Drinkwater et al. 2000a; Phillipps et al. 2001; Mieske, Hilker & Infante 2002), extremely luminous star clusters formed in galaxy interactions (Fellhauer & Kroupa 2002), low-luminosity analogues to M32 (Drinkwater et al. 2000a), and the nuclei of very low surface brightness galaxies (Phillipps et al. 2001). Fellhauer & Kroupa used numerical simulations to model the formation of star clusters that would evolve into objects similar to UCDs. Some authors have argued that highly compact galaxies might have been formed in the early Universe (Blanchard, Valls-Gabaud & Mamon 1992; Tegmark et al. 1997).

Drinkwater et al. (2000a) and Phillipps et al. (2001) argued however that the UCD luminosities, their distribution within the Fornax Cluster, and that one object was marginally resolved in ground-based imaging, implied that they were most likely to be the nuclei of tidally-stripped nucleated dwarf ellipticals (dE,Ns). Bekki, Couch, & Drinkwater (2001), building on the simulations of Bassino, Muzzio, & Rabolli (1994), modelled the tidal destruction of dE,Ns by nearby giant galaxies, calling the process tidal threshing, and predicted that the

remnants will have properties similar to UCDs.

More recently, Drinkwater et al. (2003) and Gregg et al. (2003) have presented results for the five bright Fornax Cluster UCDs using STIS imaging from the Hubble Space Telescope and high-resolution spectroscopy from the European Southern Observatory Very Large Telescope and the Keck II Telescope. All five UCDs were spatially resolved and have effective radii between 10 and 22 pc, while one was also surrounded by a lower surface brightness compact halo. These are larger than conventional globular clusters. The velocity dispersions of their stellar populations were found to be in the range 24 to 37 $\mathrm{km\,s^{-1}}$, larger than Galactic globular clusters but just overlapping the most luminous globular clusters in M31. They lie away from the globular cluster sequence in the luminosity – velocity dispersion plane, but again close to the nuclei of nucleated dwarf elliptical galaxies. Drinkwater et al. (2003) interpreted these results as supporting the hypothesis that UCDs are the remnant nuclei of threshed dE,Ns.

Bekki et al. (2003) performed detailed numerical simulations of the tidal disruption of dE,N galaxies in the vicinity of massive galaxies. They investigated the sensitivity of the disruption process to the dE,N mass, the dE,N orbital parameters and dE,N dark matter profile. Under some circumstances the disruption will be incomplete, leaving a low surface brightness halo around the dE,N nucleus. Significantly, a cuspy dark matter distribution, such as in a Navarro, Frenk & White (1996) profile, can inhibit the threshing process. Similarly, Kazantzidis, Moore & Mayer (2003) performed N-body simulations of the tidal stripping of dE,N galaxies within the core of a galaxy cluster, including the effects of baryonic matter, to quantify the stripping efficiency as a function of the concentration of Navarro-Frenk-White dark matter profiles (see also Moore 2003): complete dE,N disruption can only occur if the profiles have very low central concentrations. Thus if UCDs are indeed produced by the tidal threshing of dE,Ns, it follows that UCD observations might be a powerful test of the profiles of dark matter halos.

Recently, two further surveys of the central region of the Fornax Cluster to fainter magnitudes than the Phillipps et al. (2001) 2dF study (which extended to $b_j = 19.7$) have found a large population of fainter compact objects. Mieske, Hilker & Infante (2004) have found 54 new objects within $20'$ of NGC1399 to V = 21.0 mag (to $M_B \simeq -9.8$ mag). Meanwhile Drinkwater et al. (2004, and in preparation) have identified a similar number of compact objects to B $\simeq$ 21.5 mag extending far beyond the normal globular cluster population of NGC1399 in radial extent (as far as 0.9°), indicating that the brighter UCDs are accompanied by a much more numerous population of fainter counterparts (which will include intracluster globular clusters; see Bassino et al. 2003).

De Propris et al. (2005) compared Hubble Space Telescope imaging of the five Drinkwater et al. (2000a) Fornax UCDs with nuclei of dwarf eilliptical galaxies, finding some differences in size and surface brightness. Mieske et al. (2005) have identified candidate UCDs from HST imaging of the Abell 1689 cluster. Haşegan et al. (2005) used HST imaging and Keck telescope spectroscopy to identify compact objects in individual fields within the Virgo Cluster to investigate the relationship between UCDs and the most luminous globular clusters.

To test whether UCDs exist in other clusters, we undertook 2dF spectroscopic observations in Virgo. The central galaxies in Fornax (NGC1399) and Virgo (M87) have similar luminosities, sizes and classifications, while the two clusters have similar distributions of nucleated dwarf ellipticals (dE,Ns) in their central regions (Binggeli, Sandage & Tammann 1985; Ferguson 1989; Ferguson & Sandage 1988). The galaxy threshing model therefore predicts a population of UCDs in the vicinity of M87, yet because the Virgo Cluster is several times less dense than Fornax, one might expect fewer UCDs per volume. Although the radial distribution of the Virgo dE,Ns is slightly less concentrated than that for Fornax, there are significantly more dE,Ns in the same projected area (56 in the region covered by a two-degree diameter 2dF field centered on M87, compared to 37 for the equivalent Fornax 2dF field centered on NGC1399). Naively scaling our UCD numbers from Fornax, we expected to find 9 ± 3 UCDs in a single 2dF field centered on the M87 core of the Virgo Cluster. Bekki et al. (2003) provided more precise predictions of a population of UCDs in Virgo, using detailed N-body simulations, and demonstrated that identifying UCDs in a new environment, and measuring their detailed proper-

ties, would provide a test of formation models.

Informed by the properties of the Fornax objects, we targeted a restricted color range of unresolved objects, concentrating within 0.°65 of M87. With just 6 hours of 2dF service time we observed 1501 objects, discovering 9 Virgo UCDs within 14 to 150 kpc of M87. We report the discovery of these new UCDs in Section 2 of this paper (see also Drinkwater et al. 2004). We assume a Virgo Cluster distance modulus of 31.0 mag (see, for example, Ferarese et al. 2000), equivalent to 16 Mpc, and a Fornax Cluster distance modulus of 31.5 mag, equivalent to 20 Mpc (Drinkwater, Gregg & Colless 2001).

Since the original FCSS Fornax discoveries, we have improved the completeness in the first 2dF field and completed observations of two more. We report here, in Section 3, the discovery of one new Fornax UCD in FCSS Field 1 centered on NGC1399, and null results for the other two fields.

2. A Survey for Ultra-compact Dwarf Galaxies in the Virgo Cluster

2.1. A targetted 2dF search of the Virgo Cluster M87 core

The discovery of UCDs in the Fornax Cluster raises the questions of how common this type of object is in clusters in general, and whether the local environment in a cluster affects their number densities or properties. To address these issues, we have carried out a search for similar objects in a single 2dF field in the Virgo Cluster centered on the giant elliptical galaxy M87.

The five original 2dF Fornax UCDs were found from a nearly-complete sample of targets defined only by apparent magnitude and position, irrespective of morphology or color, at the expense of considerable observing time to obtain spectra for every such object. To improve our efficiency in Virgo, we refined our selection criteria to a subsample of unresolved (star-like) objects with colors similar to the Fornax objects. The targets were selected from the object catalog generated from United Kingdom Schmidt Telescope plates by the Automated Plate Measuring Machine (APM) in Cambridge (Irwin, Maddox & McMahon 1994; see also Maddox et al., 1990a,b). Only objects classified by the APM as being star-like (unresolved) or as merged (which includes star-like objects merged with stars or with galaxies) were chosen, to exclude obvious galaxies. Objects with physical sizes $\lesssim$ 100 pc (full-width at half-maximum) in the Virgo Cluster would be classified as unresolved. The apparent magnitude limits of the Virgo sample were set to $b_j = 16.0$ to 20.2 mag to match approximately the bright absolute magnitude limit of the FCSS in the Fornax Cluster, while extending about 1 magnitude fainter to probe more fully those objects in the Virgo Cluster with luminosities similar to the nuclei of dE,N galaxies. The Virgo targets were further constrained to have color indices $(b_j - r_F) \leq 1.6$ mag to limit their numbers, given the colors already observed for the Fornax UCDs. Imposing this color restriction reduced the number of targets by about 30% compared with a color-free sample.

A more complete sampling of targets was possible within a 0.°65 radius of M87 (72 % of the objects meeting the magnitude, colour and type criteria) and a sparser sampling (43 % in the outer part of the 2dF field (imposed by observing time constraints). This strategy produced a sample of 1501 targets in the M87 field; Figure 1 presents the color–magnitude diagrams for both the Fornax and the Virgo fields. The limits in color and magnitude used to define the two sets of targets are shown. The Virgo magnitude limits correspond to blue absolute magnitudes of $M_B = -10.6$ to -14.8 mag at the distance of the cluster. Although the areas of the Fornax and Virgo fields are identical, the respective numbers of stars differ because Fornax lies at a lower Galactic latitude, $b \simeq -54°$, than Virgo, $b \simeq +74°$.

Table 1: Virgo Cluster 2dF observations

Field center coordinates:		
Right ascension	$12^h\ 30^m\ 50^s$ (J2000)	
Declination	$+12°\ 23.''5$	
Exposures on 2dF target set ups:		
2002 April 11	55 min total	$1.''8$ seeing
2002 July 5	30 min	$1.''6$
2002 July 6	90 min	$1.''4$
2004 March 15	90 min	$1.''5$
2004 March 15	80 min	$1.''5$

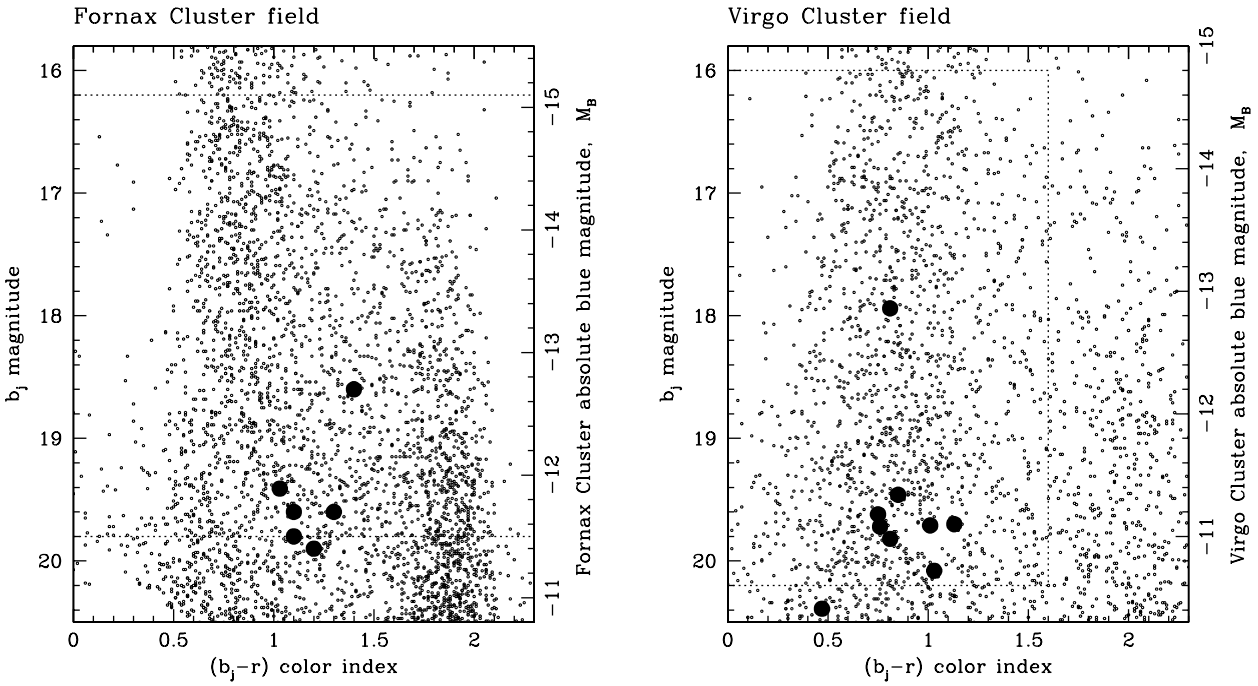

Fig. 1.— The color–magnitude diagrams for star-like objects in the Fornax and Virgo Cluster fields taken from the APM Catalog. Left: the diagram for Field 1 of the FCSS. The dotted lines show the nominal $b_j = 16.2$ and 19.8 magnitude limits on the FCSS star-like sample. The Fornax UCDs are shown as large solid circles. Right: the color–magnitude diagram for the 2dF field centered on M87 in the Virgo Cluster. The limits in color index and magnitude of the targets for the Virgo compact galaxy survey are shown by dashed lines. The Virgo UCDs described in Section 2.4 are shown as large solid circles.

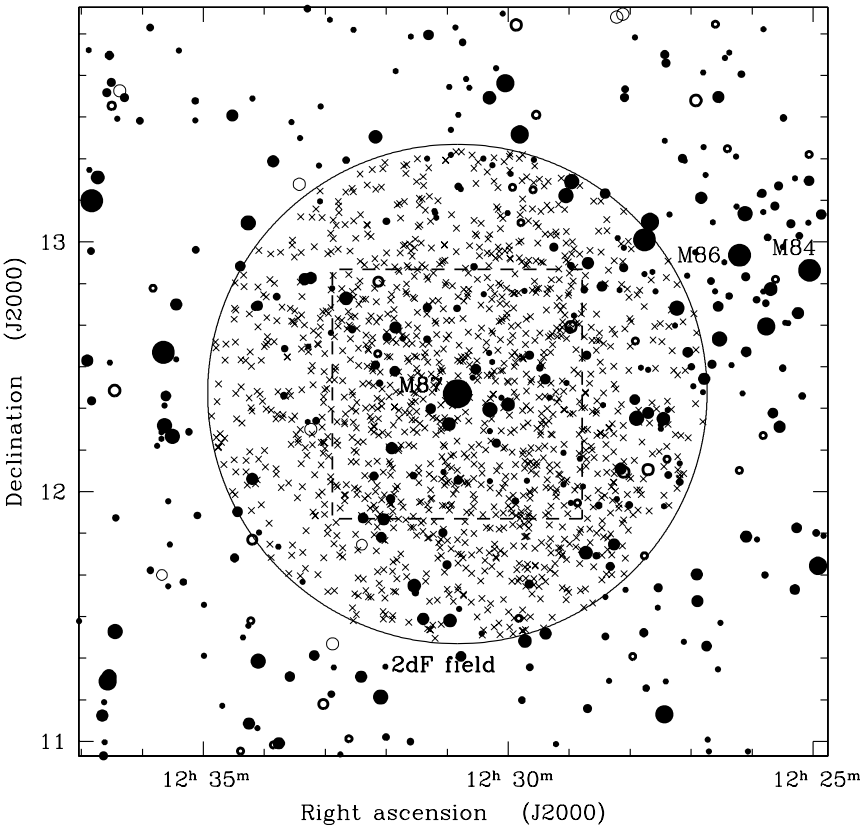

Fig. 2.— The 2dF spectrograph field of the Virgo Cluster ultra-compact dwarf survey. Galaxies from the Virgo Cluster Catalog of Binggeli, Sandage & Tammann (1985) are plotted, with cluster members shown as solid circles, possible cluster members as thick open circles, and background galaxies as thin open circles. The sizes of the galaxy symbols are scaled by apparent magnitude. 2dF targets are shown as small crosses. The dashed square delineates the region shown in Figure 3.

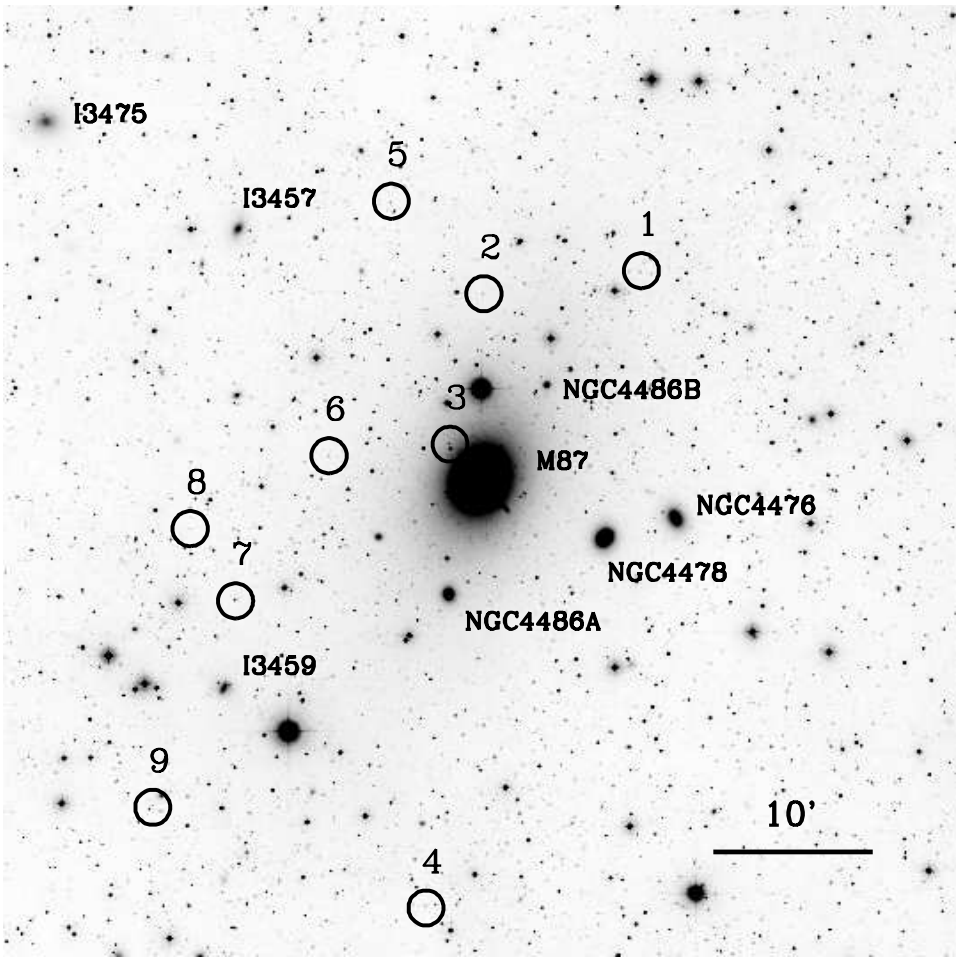

Fig. 3.— The inner 1.0 deg square region of the 2dF Virgo field, centered on M87, showing the positions of the nine ultra-compact dwarfs identified in the survey (labelled 1 to 9). North is at the top. The figure is based on a SuperCOSMOS scan of a UKST red Tech Pan film.

2.2. Observations and 2dF data reduction

AAT service observations were obtained on five separate nights for five separate 2dF set ups, totalling 6 hours of integration time. The observations are summarized in Table 1.

The 2dF spectra were obtained with the 300B grating centered at 5800Å and cover the wavelength range 3600 to 8000Å at a resolution of 9Å (FWHM). The signal-to-noise ratio is at least 10 per resolution element. The data were reduced with a combination of IRAF and the standard Anglo-Australian Observatory 2DFDR utility (Bailey, Glazebrook & Bridges 2002). As is normal for 2dF data, arc lamp exposures and fiber flats were recorded, but no sky frames or dark-current exposures. Each spectrum was wavelength calibrated but not flux calibrated. After reduction with 2DFDR, IRAF was used to correct any spectra suffering from poor quality sky background subtraction after the automated reduction by 2DFDR. IRAF was also used to remove cosmic ray event detections. Splitting integrations into a few different exposures allows most cosmic rays to be eliminated from the coadded data.

2.3. Data analysis

Radial velocities were determined through cross-correlation with an array of template spectra representing an emission-line galaxy, a quasar, and nine different types of star (having spectral types from A3V to M5V to provide a match both to stars and early-type galaxies). This was done within the RVSAO IRAF package (Kurtz & Mink 1998). The template giving the highest R coefficient (Tonry & Davis 1979) provides the adopted radial velocity for an observed spectrum, as well as a simple indication of the type of spectrum. Further details of the observing and reduction were given in Drinkwater et al. (2000b) and Deady et al. (2002).

When a target has been observed more than once, which does sometimes occur because of fiber positioning practicalities, the result having the highest R coefficient is adopted. Only results having $R \geq 3.0$ are considered reliable.

2.4. Discovery of ultra-compact dwarfs in Virgo

A total of 1633 spectra were obtained of 1501 individual targets. Of these, 1322 had reliable ($R \geq 3.0$) velocity results. These results were obtained for 60% of objects satisfying the object type, magnitude and color constraints over the whole 2dF field, and for 70% within $0\overset{\circ}{.}65$ of M87. Figure 4 presents the histogram of heliocentric radial velocities for objects in the range -500 to 2200 kms^{-1}. The distribution is dominated by Galactic stars between -200 and 400 kms^{-1}. Ten objects have radial velocities between 400 and 2100 kms^{-1}. One of these (at $12^{\rm h}\ 31^{\rm m}\ 54\overset{\rm s}{.}84$, $+11^\circ$ 56' $59\overset{\prime\prime}{.}6$, J2000) gave a velocity of 527 ± 121 kms^{-1} and its strongest cross-correlation result is with the A-type stellar template. This object is more likely to be a Galactic star, given the formal overlap of its velocity with the velocity distribution of Galactic stars and the relatively early spectral type of its best match template spectrum.

About 10% of already known Virgo members within our survey area have radial velocities $<$ 400 kms^{-1}; some even have negative radial velocities. Thus a consequence of applying a low-velocity cut-off to avoid Galactic star contamination in the compact object sample is that the survey may miss UCDs with radial velocities below 400 kms^{-1}. We estimate that there may be 1 ± 1 additional UCDs among the objects observed that has been lost by applying this cutoff (assessed by applying this cut-off to the distribution of observed UCD velocities). But UCDs with $cz <$ 400 kms^{-1} will be very difficult to distinguish from Galactic stars, especially with poorly flux calibrated fiber spectra, so obtaining a dynamically complete sample of Virgo UCDs will prove difficult with currently available observing resources.

We identify as UCDs the remaining nine objects with velocities consistent with Virgo Cluster membership. Like those in Fornax, all nine Virgo UCDs have early-type galaxy spectra. Most were fitted best by stellar templates of K- or M-type solar-composition stars, consistent with old, moderately metal-rich stellar populations. The spectrum of Virgo UCD 4, however, shows a bluer continuum (Figure 5) and the best fitting tem-

TABLE 2

NEW 2DF ULTRA-COMPACT DWARFS IDENTIFIED IN THE VIRGO AND FORNAX CLUSTERS

Object	IAU name	R.A. h m s	Dec. ° ′ ″	b_j mag	$(b_j - r)$ mag	R coeff.	cz (kms^{-1})	Best template
Virgo UCD 1	J123007.6+123631	12 30 07.61	+12 36 31.1	19.6	0.8	5.2	1103 ± 114	M1V
Virgo UCD 2	J123048.2+123511	12 30 48.24	+12 35 11.1	19.7	1.0	7.4	824 ± 50	K5V
Virgo UCD 3[1]	J123057.4+122544	12 30 57.40	+12 25 44.8	19.5	0.9	9.9	698 ± 40	K5V
Virgo UCD 4	J123104.5+115636	12 31 04.51	+11 56 36.8	19.7	0.8	8.0	824 ± 46	G0V
Virgo UCD 5	J123111.9+124101	12 31 11.90	+12 41 01.2	19.7	1.1	7.3	1159 ± 45	K5V
Virgo UCD 6	J123128.4+122503	12 31 28.41	+12 25 03.3	19.8	0.8	6.4	2041 ± 63	M1V
Virgo UCD 7	J123152.9+121559	12 31 52.93	+12 15 59.5	17.9	0.8	6.1	790 ± 65	K5V
Virgo UCD 8	J123204.3+122030	12 32 04.36	+12 20 30.7	20.4	0.5	3.5	1607 ± 68	K5V
Virgo UCD 9	J123214.6+120305	12 32 14.61	+12 03 05.4	20.1	1.0	4.9	1216 ± 61	K5V
Fornax UCD 6	J033805.0−352409	03 38 05.08	−35 24 09.6	19.4	1.0	11.2	1212 ± 32	K5V

The properties of the new bright UCDs identified with 2dF are listed. The J2000 celestial coordinates are from the APM catalog. The APM b_j magnitude is on the photographic blue (IIIa-J + GG395) photometric system. The APM photographic $(b_j - r)$ color index is accurate to ±0.3 mag. R is the Tonry & Davis R coefficient. cz is the heliocentric radial velocity. The best template is the template spectrum used in the cross-correlation that gave the highest R coefficient.

[1] Virgo UCD 3 is object 547 in the study of the M87 globular cluster system by Strom et al. (1981).

plate was that of a G0-type star, which can be explained by stellar populations that are younger or more metal-poor than the other UCDs. The objects are listed in Table 2.

A check of positions confirmed that none coincided with any known cluster galaxies in the Virgo Cluster Catalog (Binggeli, Sandage & Tammann 1985), although UCD3 lies close to M87. None of the UCDs matches the objects described by Haşegan et al. (2005), who studied specific fields within the Virgo Cluster. While there are Haşegan et al. objects within our 2dF field, all their confirmed Virgo Cluster compact objects are located within 6' of M87, whereas the UCDs reported in this paper lie between 3' and 29' of M87.

Eight of the nine were classified in the APM Catalog as being stars on both the blue and red sky survey plates. The exception was UCD number 7 which was classified as a galaxy from the red plate and a merged object on the blue. This object appears on available imaging data to have a number of nearby images which confuses its classification: this is discussed in more detail in Sections 2.5 and 2.9.

2.5. Surface brightness profiles

The UCDs are mostly star-like in the APM Catalog (one is a "merged" object). Better quality imaging data are therefore needed to attempt to resolve their surface brightness profiles. Phillipps et al. (2001) found that one of five Fornax Cluster ultra-compact dwarfs was resolved in Schmidt photographic images. Using imaging from the Hubble Space Telescope, Drinkwater et al. (2003) showed that this object (Fornax UCD 3) consists of a highly compact core within a more extended envelope. Resolving the Virgo UCDs is important for comparing them to the Fornax sample and to further test models of their origin. Bekki et al. (2003), for instance, predict that under some circumstances in the dE,N tidal threshing model, residual halos can remain around UCDs.

We have used CCD data from the Isaac Newton Telescope Wide-Field Survey (INT WFS) of the Virgo Cluster (Trentham & Hodgkin 2002) to measure the surface brightness profiles of the Virgo UCDs. Blue (B band) data have been selected because of the greater depth and generally flatter background than the corresponding ultra-

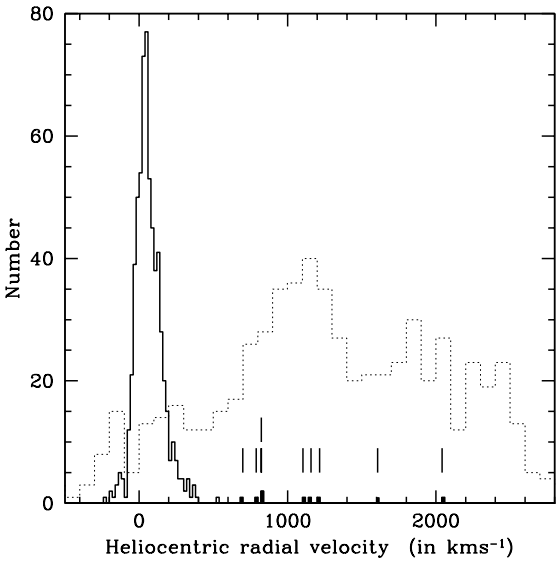

Fig. 4.— The histogram of velocities for the 2dF targets having $R \geq 3.0$ showing Galactic stars (solid line) and Virgo Cluster UCDs (solid areas, and also indicated by vertical lines). For comparison, the dotted line shows the velocity distribution for galaxies in the Binggeli, Sandage & Tammann (1985) Virgo Cluster Catalog across the entire cluster using radial velocity data in the NASA Extragalactic Database.

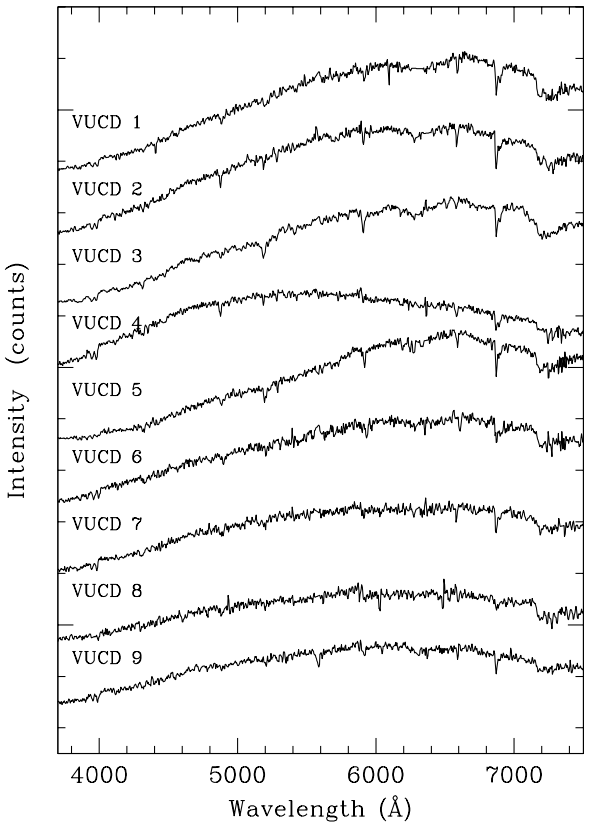

Fig. 5.— Spectra of the nine Virgo Cluster UCDs obtained with the 2dF spectrograph.

violet or infrared data. Each UCD has been imaged in more than one B band exposure, so we have selected just the best-seeing B band exposures to measure the light profiles. Comparing the UCD surface brightness profiles with stars from the same images shows no strong evidence that any of the UCDs are resolved, although UCDs 4 and 7 hint at being marginally extended in the profiles. Table 3 summarises the object size data. UCD7 appears extended in the wings of its profile only and therefore does not appear extended in Table 3.

Figure 6 shows images of the Virgo UCDs created from a very deep stack of photographic films of the M87 region recorded with the UKST. The data were produced by the SuperCOSMOS Sky Unit at the Royal Observatory Edinburgh by coadding digitized scans of 63 red filter exposures on Tech Pan emulsion (see Phillipps et al. 1998 for a discussion of this type of data). The point-spread function in the coadded data is $2.5''$, poorer than the available INT CCD data; however, the photographic data have a much greater depth and uniform quality. These data are discussed in further detail in Sections 2.9 and 2.10.

Virgo UCD 6 has three compact objects $6''$ just to the north, northeast and east in the INT B band and infrared (i band) images: see Figure 12, which presents a B-band image of UCD 6 recorded in a 25-minute integration with the Wide-Field Camera on the 2.5-metre Isaac Newton Telescope in La Palma. These three objects lie 6 to $7''$ from the UCD, which corresponds to a projected distance of about 500 pc in the Virgo Cluster. Two of them are compact, while the third is resolved and is elongated. They appear as two objects in the lower resolution UKST photographic data. It is not clear from the imaging data whether these are three background/foreground objects or whether they are possible debris from the tidal stripping of a progenitor galaxy (see also Sections 2.9 and 4). The 2dF spectrum, given the fiber-fed character of 2dF, included light from only the UCD and not the companion objects. The compact images appear bluer by 0.3 mag than the UCD in (B-i), while the elongated image is redder by 0.4 mag. There is no obvious evidence of discrete structures around any of the other UCDs. Section 2.9 below discusses limits on halos around the UCDs.

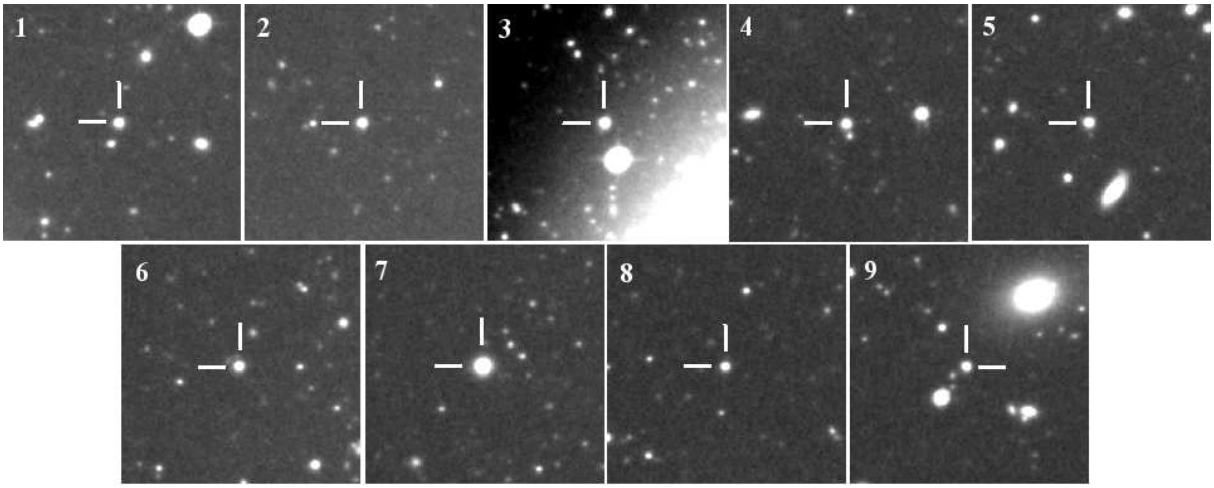

Fig. 6.— Images of the nine Virgo Cluster UCDs from the stack of 63 UKST red band films. Each frame is 2′.0 wide and north is at the top. The UCD is centered in each frame.

Table 3: Images sizes for the Virgo UCDs in INT CCD data

Virgo UCD	Frame seeing (″) (±0″.1)	UCD size (″) (±0″.2)
1	1.8	1.8
2	1.4	1.6
3	1.1	1.3
4	1.9	2.4
5	1.1	1.2
6	1.0	1.2
7	1.1	1.3
8	1.5	1.1
9	1.6	1.8

The object sizes of the UCDs in CCD data from the Isaac Newton Telescope are compared with the mean sizes of stars.

2.6. The luminosities of the UCDs

Figure 7 presents a histogram of the B band absolute magnitudes for the UCDs, as computed from the apparent magnitudes using an apparent (reddening uncorrected) Virgo Cluster distance modulus of 31.0 mag. Note that absolute magnitudes are expressed here for the B band, converted from the b_j photographic apparent magnitudes using a color typical of evolved stellar populations. The absolute magnitudes range from $M_B = -12.9$ to -10.7, while the survey limits were $-14.8 \leq M_B \leq -10.6$. These are comparable to the luminosities of the six bright Fornax UCDs ($M_B = -13.8$ to -11.6, with survey limits of -15.1 to -11.5). In both clusters, the UCDs so far identified have luminosities towards the fainter end of the range explored with 2dF. This suggests that the peak in the Virgo UCD luminosity function could lie at $M_B > -12$, and possibly fainter than the faint limits of the survey, predicting larger numbers of these objects at fainter levels (as has been found to be the case in Fornax), subject to confusion with any intracluster globular clusters. .

Figure 7 also shows the luminosity functions of other objects in the Virgo Cluster. Comparisons are possible with the nuclei of dE,N galaxies, which overlap with the UCD luminosities at the luminous end of the nucleus distribution. This result is similar to that of Drinkwater et al. (2000a) for

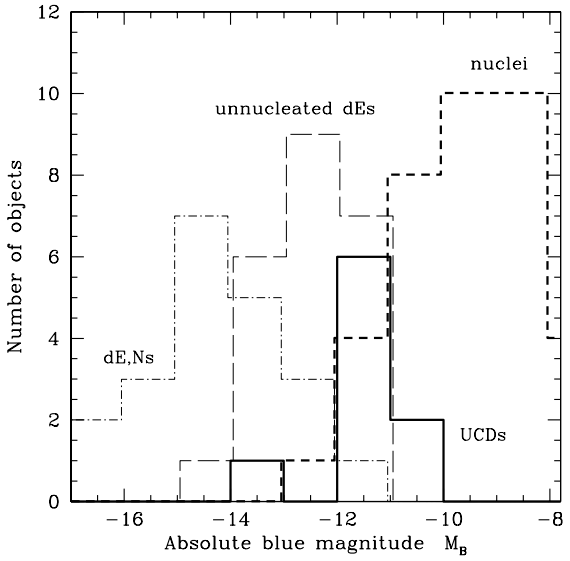

Fig. 7.— The luminosity function of the Virgo UCDs compared with other objects in the Virgo Cluster. The distribution of absolute magnitudes of the UCDs is shown as a bold solid line. Total absolute magnitudes of nucleated dwarf elliptical (dE,N) and non-nucleated dwarf elliptical galaxies were taken from data in the Virgo Cluster Catalog (Binggeli, Sandage and Tammann 1985). These are presented for those galaxies lying within 0.°6 of M87 only, to allow a direct comparison with the UCDs. The absolute magnitudes of the nuclei of Virgo dE,N galaxies are taken from Lotz, Miller & Ferguson (2004) and from Durrell (1997).

Fornax UCDs. A direct comparison of the numbers of UCDs and Virgo dE,N nuclei cannot, however, be made because of the heterogeneous samples of dE,N nuclei that have reliable nuclear magnitudes in the literature. Figure 7 shows the total luminosities of dE,N and non-nucleated dE galaxies within the same projected radial distance (0.°6) of M87 as the UCDs. The numbers of dE,Ns, dEs and UCDs can be compared directly.

2.7. The distribution of the UCDs within the Virgo Cluster

Figure 9 presents the cumulative distribution of the Virgo UCDs as a function of radial angular distance from M87. All of the Virgo UCDs lie within 0.°6 of M87 (projected distance of 170 kpc), though this might be due in part to the sparser sampling of targets outside this radius. Half of the UCDs lie within 0.°3 (80 kpc) of M87.

Figure 9 also compares the angular distribution of the UCDs with those of non-nucleated and nucleated dwarf ellipticals (taken from the Virgo Cluster Catalog of Binggeli et al. 1985), normalized to match the number of UCDs within 0.°5 of M87 (the maximum radial distance found for the UCDs). There is a moderate match between the UCD distributions and the two types of dwarf ellipticals. However, dwarf ellipticals are found across the cluster and this result depends critically on the radius used for the normalization. A Kolmogorov-Smirnov test shows that the distribution of non-nucleated dwarf ellipticals normalized within 0.°5 of M87 matches that of the UCDs with a 32% probability. The sparser sampling of 2dF targets beyond 0.°6 of M87 does not affect this result.

A direct comparison of the distribution of UCDs with the M87 globular cluster system is more difficult given the restricted range in radii covered by past surveys of the M87 globular cluster system. For example, the study of McLaughlin et al. (1994) covers radii out to 9′: in that study, 50% of globular clusters are found within 3′ of the centre of M87. In contrast 50% of the Virgo UCDs of Table 2 lie within 17′ of M87, while only one of the nine lies within 9′.

2.8. Virgo UCD dynamics

The mean heliocentric radial velocity of the nine UCDs is 1051 ± 139 kms^{-1} (weighted according to the errors given by the RVSAO software), with a dispersion of 416 ± 110 kms^{-1}. Interpretation of these results is slightly complicated by the lower velocity cut-off at 400 km s^{-1} that was imposed on the compact-object sample to reject Galactic stars.

The sample of Virgo UCDs is too small for definitive conclusions to be made about whether their systemic velocity is consistent with that of M87 (having a heliocentric radial velocity of 1307 ± 7 km s^{-1} in the NASA Extragalactic Database, NED)[1], with that of dE,N galaxies in the vicinity of M87, or with that of the M87 globular cluster system. Differences in the mean velocity and the velocity dispersion might provide tests of the origin of the UCDs. The mean velocity and dispersion of the UCDs are statistically different to the entire sample of cluster galaxies close to M87 (there are 37 galaxies with NED velocities between 400 and 3500 km s^{-1} lying within 1.°0 of M87; these have a mean velocity of 1402 ± 105 kms^{-1} and a velocity dispersion of 639 ± 75 kms^{-1}). The larger velocity dispersion of the general galaxy population than that of the UCDs parallels the results for Fornax UCDs by Mieske, Hilker & Infante (2004); but this conclusion depends on imposing a lower velocity limit of 400 km s^{-1} on cluster galaxies so that the samples have similar velocity selection criteria.

2.9. Limits on low surface brightness halos around the UCDs

Phillipps et al. (2001) showed that one of their Fornax UCDs was resolved in ground-based imaging. Using numerical simulations, Bekki et al. (2003) showed that dE,N nuclei might be only partially stripped in their threshing model, leaving a halo around a UCD. The existence of faint halos around any of the Virgo UCDs might provide important information about formation mechanisms.

The deep stack of UKST photographic films produced by the SuperCOSMOS Unit, described in Section 2.5, was used to place limits on emission within 8″ of the UCDs, above that expected from a point-spread function. The pixel-to-pixel variation in the sky background is at the 26.3 R mag arcsec^{-2} level and R = 23.5 mag point sources are detected with a signal-to-noise ratio of 5. A circular annulus having an inner radius of 5″ and an outer radius of 8″ (corresponding to a transverse linear distances of 390 and 620 pc in the Virgo Cluster) was centered on each UCD and the signal in the annulus recorded. The inner radius is set by the point-spread function: 6% of the light of a point source spills into this annulus (measured from images of stars). The full-width at half-maximum of the point-spread function is 2.5″; this figure is uniform across the region where the UCDs are located. Some discrete objects in the vicinity of the UCDs were masked before making the measurements. This did not include the objects very close to UCD 6, and the procedure may have been incomplete for UCD 7 which had several objects within 20″.

Table 4 presents 2.5σ limits on the detection of emission in the annuli above that from the point-spread function. These are expressed as the mean magnitude surface brightness in the annuli corresponding to a 2.5σ deviation above the sky background level after applying a correction for light spilling from the UCD. A significant contribution to the error is the uncertainty in the point-spread function (5.6 ± 1.1% of the UCD light is expected to spill into the annulus, based on tests on images of stars).

There is a formal detection of excess light around two UCDs. However, one of these (number 6) has the three discrete contaminating sources within 6″ from the UCD center (discussed in Sections 2.5 and 4). The other (number 7), as discussed above, also has several additional sources within 20″ and some within 10″. Although these objects were masked, some residual signal may still contaminate the annulus. It is therefore not possible to claim with confidence any evidence of extended halos around any of the Virgo UCDs.

2.10. Might the UCDs be the nuclei of very low surface brightness dE,Ns?

It is important to rule out the possibility that the UCDs are merely the high surface brightness, compact nuclei of dE,N galaxies with lower

[1]The NASA/IPAC Extragalactic Database is operated by the Jet Propulsion Laboratory, California Institute of Technology, under contract with the National Aeronautics and Space Administration.

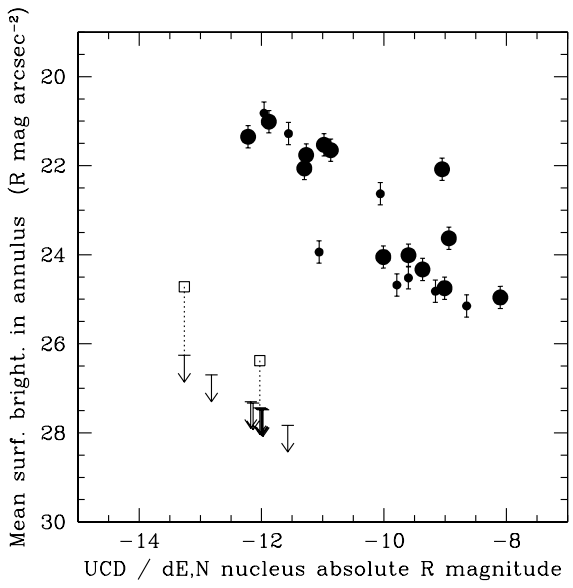

Fig. 8.— A comparison of the 2.5σ surface brightness limits on extended halos around the Virgo UCDs with the detections of dE,N galaxies when the same analysis is performed on dE,N nuclei. The 2.5σ limits on the signal in the circular annuli of Section 2.9 are plotted against the UCD absolute magnitudes and are shown as arrows. The two UCDs (numbers 6 and 7) that gave formal detection are shown by squares, alongside their respective 2.5σ limits: the reliability of these two detections are discussed in Section 2.9. Equivalent data for Virgo (large circles) and Fornax (small circles) dE,N galaxies are shown for comparison, in the form of the mean surface brightness in 5 to 8 arcsec radius annuli centered on the nucleus plotted against nucleus absolute magnitude. Section 2.10 discusses the comparison of UCDs with dE,Ns in more detail.

than average surface brightness halos. Phillipps et al. (2001) and Drinkwater et al. (2003) compared limits on the surface brightnesses of extended light around Fornax UCDs in relation to surface brightness data for dE,N galaxies. Their analyses showed that their five Fornax UCDs were different in character to ordinary dE,N galaxies.

This analysis is repeated here for the nine Virgo UCDs. The 5 to 8″ annuli used in Section 2.9 were applied to a sample of Virgo dE,N galaxies, using the same stack of UKST films as for the UCD analysis. This provided mean surface brightnesses within 5 to 8″ of the nuclei of the dE,N galaxies: all are easily detected. Figure 8 shows the mean surface brightness in the annuli plotted against the magnitude of the nucleus of the dE,N. Errors are estimated to be ±0.2 mag. We used the best nuclear magnitude estimates from the literature, derived from high-resolution imaging (see the discussion of Binggeli & Cameron 1993 about the difficulties of measuring nuclear magnitudes from photographic data). The nuclear magnitudes from the HST WFPC2 study by Lotz, Miller & Ferguson (2004) were converted to R-band absolute magnitudes (for our adopted Virgo distance modulus of 31.0 mag, and using a transformation $(V-R)_C = 0.52\,(V-I)_C$ based on data given by Bessell (1979) for solar-composition main sequence stars). One dE,N nucleus was rejected from this analysis: VCC1714 has a nuclear color from Lotz, Miller & Ferguson (2004) that is 5.3 standard deviations from the mean of the other 29 nuclei in their study, and it is displaced off-center to an unusual degree in the galaxy image. We reject VCC1714 on the basis that it is an unusual object or that its "nucleus" may be a Galactic star (but see, for example, De Rijcke & Debattista 2004 for a discussion of off-center nuclei). This sample of Lotz, Miller & Ferguson galaxies was supplemented by data for one galaxy (VCC1783) from Lotz et al. (2001), and from the ground-based CCD study of Durrell (1997) for 3 galaxies, giving a total of 14 Virgo dE,Ns within the region of the SuperCOSMOS scans.

These Virgo dE,N galaxy results were supplemented by an analysis of a SuperCOSMOS scan of a single UKST film on Tech Pan emulsion of the center of the Fornax Cluster. This provided data for a further 8 dE,Ns with nuclear magnitudes from Lotz et al. (2001). The Fornax results

are shown as small circles in Figure 8, while the Virgo dE,Ns are shown as large circles. The Virgo galaxies show the same surface brightness – nucleus magnitude correlation as the Fornax galaxies.

Figure 8 also shows the 2.5σ limits for the non-detections of seven Virgo UCDs, with the formal detections for the other two UCDs. These are plotted against the R band absolute magnitudes of the UCDs, allowing a direct comparison to be made with the dE,N galaxies, in a similar manner to the Fornax analysis of Drinkwater et al. (2003). The correlation for the UCDs between surface brightness limit and magnitude is caused by the error in surface brightness introduced by uncertainties in the point-spread function. (In contrast, the contribution of nucleus light into the annulus around dE,Ns, at $0-8$ %, is negligible compared to the light of the main body of the galaxy.) The limits for the UCDs are displaced from the locus of the dE,N galaxies by 5–6 magnitudes in surface brightness. On this basis we dismiss the hypothesis that UCDs are the nuclei of dE,N galaxies of lower than average surface brightness.

3. Ultra-compact Dwarf Galaxies in the Fornax Cluster

3.1. The Fornax Cluster Spectroscopic Survey

The Fornax Cluster Spectroscopic Survey (FCSS) has aimed to obtain spectra with the 2dF spectrograph of all objects having blue photographic magnitudes between $b_j = 16.5$ and 19.7 in the direction of the Fornax Cluster (see Drinkwater et al. 2000b for a description of the survey and Phillipps 1997 for the original strategy). Deady et al. (2002) have already described the results for dwarf galaxies in the cluster core from the first of the 2dF fields (for B-band absolute magnitudes mostly in the range -11.6 to -14.8). The 2dF fields used in the survey are shown in Figure 11.

The five UCDs reported by Drinkwater et al. (2000a) and Phillipps et al. (2001) were discovered in the first FCSS field at a time when 86% of the star-like targets in that field had been observed between magnitude limits at $b_j = 16.2$ and 19.8. The magnitude limits for the star-like targets was slightly broader than the nominal $b_j = 16.5$ to 19.7 limits of the overall survey. Since then the completeness of Field 1 has been improved by further observations and Fields 2 and 3 have been observed. Details of the fields are presented in Table 5. Velocities have now been measured for 92% of the Field 1 star-like objects to $b_j = 19.8$ and some targets have been observed to $b_j = 20.0$. The non-detection of UCDs in Fields 2 and 3 is discussed in Section 3.3.

3.2. Fornax UCD6: A bright ultra-compact dwarf in FCSS Field 1

Only one UCD has been found in the Fornax Cluster from the FCSS observations in addition to the five reported by Drinkwater et al. (2000a) and by Phillipps et al. (2001). Its position and color have previously been described by Karick, Drinkwater & Gregg (2003), who found V=18.9, (B-V)=0.8, $(V-I)_C$=1.2, and an independent velocity measurement and color have been reported by Mieske, Hilker & Infante (2004). The properties of UCD6 are summarized in Table 2. The object has a blue photographic apparent magnitude $b_j = 19.3$, equivalent to a blue absolute magnitude $M_B = -12.0$, comparable to those of the first five UCDs. The best-fitting cross-correlation template spectrum is that of a K5 star, again similar to the first five UCDs. UCD6 lies only $6'$from the giant elliptical galaxy NGC1399, equivalent to a projected distance of 35 kpc, whereas the entire distribution of bright UCDs extends as far as $28'$(170 kpc).

Figure 10 shows the radial light intensity profile of the new Fornax Cluster UCD determined from a SuperCOSMOS plate measuring machine scan of a red photographic film recorded with the United Kingdom Schmidt Telescope (UKST) on Technical Pan emulsion (Parker & Malin 1999, Schwartzenberg, Phillipps & Parker 1995). It is compared with the mean profile of star images from the same scan, and with the profiles for the five UCDs presented by Phillipps et al. (2001). The UCD is not obviously resolved in the photographic data (with a 2.3 arcsec seeing disc), unlike the third of the Drinkwater et al. (2000a) objects.

Karick, Drinkwater & Gregg (2003) published photometry for an additional object found during a preliminary analysis of 2dF data (which they labelled UCD7). A detailed analysis has failed to confirm this as a Fornax Cluster object. It appears to be a Galactic star which gave a double peak in

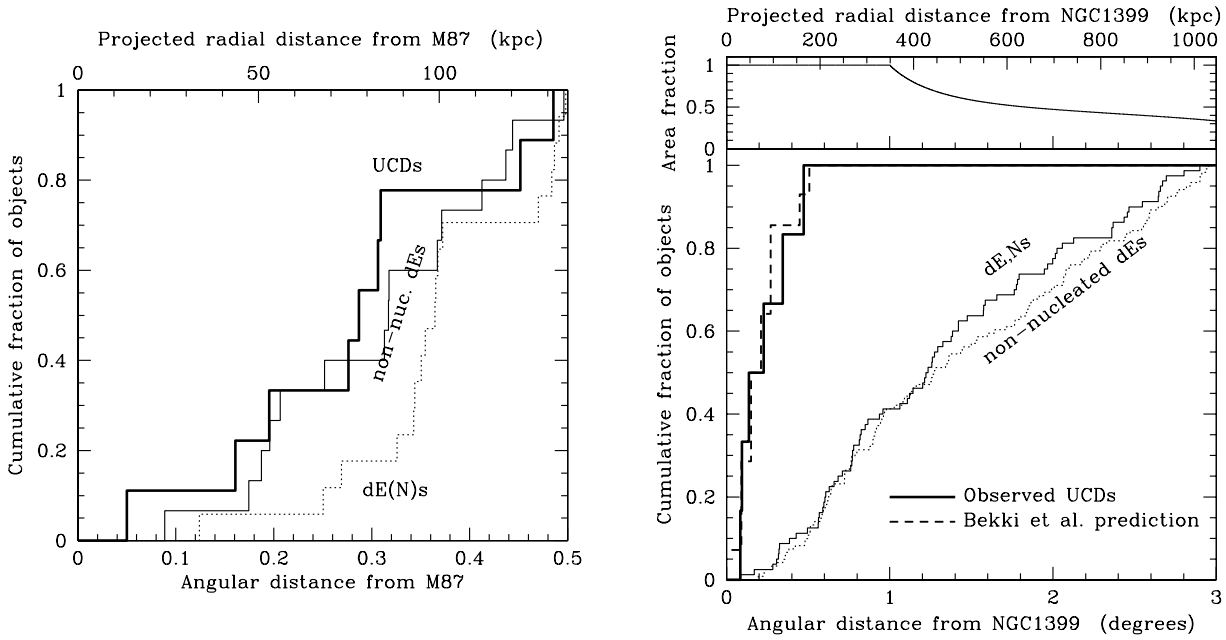

Fig. 9.— Left: The radial distribution of the nine Virgo ultra-compact dwarfs. The number of UCDs found within a particular angular distance of M87 is plotted against the angular distance. The distributions of nucleated dwarf ellipticals (dE,Ns) and non-nucleated dwarf ellipticals are presented, taken from the Virgo Cluster Catalog of Binggeli, Sandage & Tammann (1985) and normalized so that the numbers of galaxies within $0\overset{\circ}{.}5$ of M87 match the numbers of UCDs. Right: The radial distribution of the six Fornax ultra-compact dwarfs found in the FCSS, covering the full 3 degree radius of the survey. The cumulative number of UCDs found within a particular angular distance of NGC1399 is plotted against the angular distance, compared with the distribution of UCDs predicted by Bekki et al. (2003) on the basis of the tidal threshing model. The distributions of nucleated dwarf elliptical (dE,N) and non-nucleated dwarf elliptical galaxies are shown, taken from the Fornax Cluster Catalog of Ferguson (1989). The top panel shows the cumulative fraction of the area of sky surveyed by the FCSS as a function of distance from NGC1399.

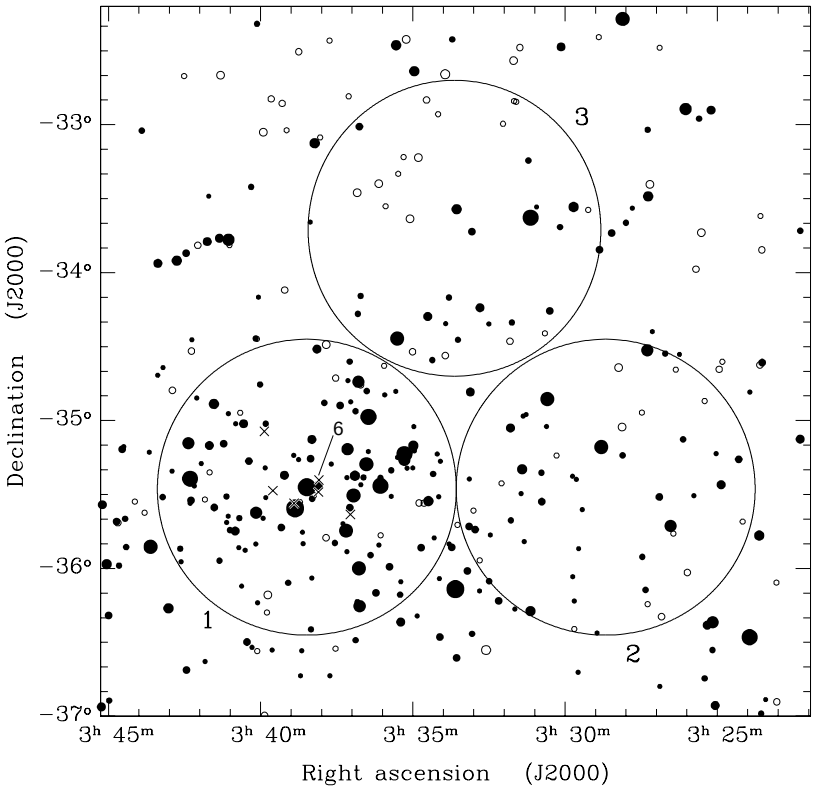

Fig. 11.— Fields 1, 2 and 3 of the Fornax Cluster Spectroscopic Survey showing the galaxies from the Fornax Cluster Catalog of Ferguson (1989). The 2dF spectrograph fields of the Fornax Cluster Spectroscopic Survey (see also Drinkwater et al. 2000b) are drawn as circles and are numbered. The definite or likely cluster members of the Fornax Cluster Catalog are plotted as solid points, and possible cluster members as open circles. The sizes of the symbols are scaled by apparent magnitude. The six bright UCDs detected in the FCSS are shown as crosses, and UCD 6 is labelled.

Table 4: Limits on halos around the Virgo UCDs

Virgo UCD	2.5σ limit above sky level (R mag arcsec^{-2})	Mean surface brightness if above 2.5σ limit (R mag arcsec^{-2})
1	27.5	–
2	27.5	–
3	26.7	–
4	27.3	–
5	27.3	–
6	27.4	26.4 ± 0.2
7	26.3	24.7 ± 0.1
8	27.8	–
9	27.5	–

The mean surface brightnesses and limits are presented for circular annuli with inner and outer radii of 5 and 8 arcsec centered on the UCDs. The results represent the signals in the annuli after corrections for light spilling from the point-spread function of the UCDs.

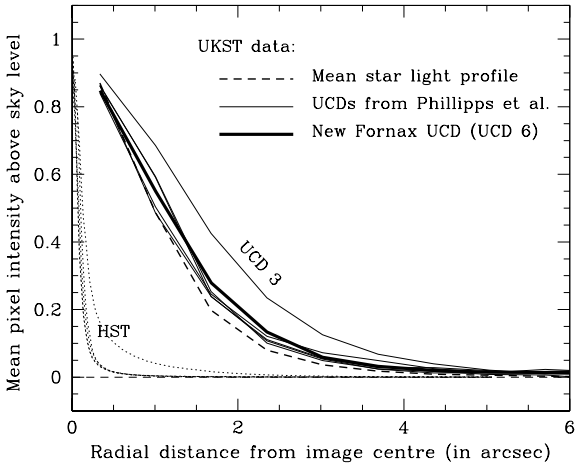

Fig. 10.— Radial light intensity profiles for Fornax Cluster UCD6 derived from a SuperCOSMOS scan of a UKST red Tech Pan film. The profiles of the five UCDs of Drinkwater et al. (2000a) and a mean star point-spread function from the same UKST data are shown for comparison, taken from Phillipps et al. (2001). Resolved profiles from the Hubble Space Telescope STIS data of Drinkwater et al. (2003) are shown for the first 5 UCDs to illustrate the effects of seeing on the UKST images.

Table 5: New Fornax Cluster 2dF observations

Fornax Cluster Spectroscopic Survey fields :

Number	Field center coordinates (J2000) Right ascension	Declination
Field 1	$03^{\rm h}\ 38^{\rm m}\ 29.0^{\rm s}$	$-35^\circ\ 27'\ 01''$
Field 2	03 28 40.0	−35 27 01
Field 3	03 33 38.0	−33 41 59

Each field is 2.°0 in diameter.

the cross-correlation function.

3.3. No ultra-compact dwarfs in FCSS Fields 2 and 3

In contrast to the six UCDs in the first of the FCSS 2dF fields, no such objects have been found in Fields 2 or 3 despite similar selection criteria and survey completeness as Field 1. While Field 1 is centered on NGC1399 and the cluster core, these two new 2dF fields do still contain numerous Fornax Cluster galaxies, both giant and dwarf. We emphasize again that despite surveying out to a distance $\simeq 1$ Mpc, all the UCDs detected in the FCSS are inside a radius of 170 kpc of the cluster center. This is strong evidence that UCDs are a phenomenon associated with dense environments in clusters.

3.4. Properties of the Fornax ultra-compact dwarfs

The new Fornax object increases the sample of bright ($b_j \leq 20.0$ mag) Fornax Cluster UCDs to a total of six. All six lie within $28'$ of NGC1399.

Figure 9 shows the distribution of the Fornax UCDs with angular radius from NGC1399 (the prominent central elliptical galaxy of the Fornax Cluster) in the form of a cumulative number distribution. The figure covers the entire radial extent of the 2dF survey, extending to 3.0 deg from NGC1399, although the area sampling becomes progressively incomplete at larger radial distances because of the geometry of the 2dF fields. Nevertheless, the figure illustrates clearly the cut-off in the UCDs at 0.5 deg, equivalent to a projected angular distance of 170 kpc. The distribution of UCDs predicted by Bekki et al. (2003) using the tidal threshing hypothesis for an age of 8.5 Gyr is shown for comparison (see also their Figure 9). There is a close match between the shapes of the distributions. However, Bekki et al. predict 14 UCDs formed from the disruption of nucleated galaxies, significantly larger in number than the 6 found in the FCSS. This is smaller than the 59 faint objects found by Mieske, Hilker & Infante (2004), but their sample will include many conventional globular clusters. The FCSS sample limits at faint magnitudes mean that fainter remnant nuclei of dE,Ns would be overlooked had the UCDs been created by the tidal threshing process. Luminosity information for dE,N nuclei (e.g. Lotz et al. 2001) suggests that a majority of the Bekki et al. predicted UCDs would not get into the 2dF sample (given that the threshing model predicts a luminosity function that matches the nuclei), broadly in line with the observed numbers.

Figure 9 also shows the distribution of nucleated and non-nucleated dwarf elliptical galaxies. It should be noted, however, that the numbers of these galaxies (90 and 138) are very much larger than the number of UCDs. For example, within 0.5 deg of NGC1399, there are 10 dE,Ns and 13 non-nucleated dEs.

The mean heliocentric radial velocity of the six bright Fornax UCDs is $1460 \pm 109\,\mathrm{kms}^{-1}$ on the basis of the 2dF data, with a standard deviation of $266 \pm 78\,\mathrm{kms}^{-1}$ (including the effects of observational errors). The heliocentric radial velocity of NGC1399 from the NASA Extragalactic Database is $1425 \pm 4\,\mathrm{kms}^{-1}$. There is therefore no evidence from the 2dF data alone that the six bright UCDs have a different systemic velocity to NGC1399. Mieske, Hilker & Infante (2004) reported a slightly higher velocity for brighter UCDs than for NGC1399 (and also than for fainter compact objects). There is a mean difference of only $20 \pm 34\,\mathrm{km\,s}^{-1}$ between the Mieske et al. and 2dF results (for 5 objects in common).

4. Discussion

None of the 9 Virgo objects shows clear evidence of being resolved in ground-based CCD imaging or of having extended low surface brightness halos, but Virgo UCD 4 appears slightly larger than the seeing disc in the best seeing exposure available (and incidentally has a bluer continuum in its spectrum than the other 8 UCDs). Of all 15 bright UCDs across both clusters, only Fornax UCD 3 is unambiguously resolved in ground-based imaging (which was discussed in detail by Drinkwater et al. 2003). The failure to find strong evidence of spatially extended emission around the UCDs (beyond $5''$) indicates that they are unlikely to be the nuclei of dE,N galaxies which simply have extremely low surface brightness halos, given the observed correlation between the surface brightnesses of dE,Ns and nuclear magnitudes presented in Section 2.10 (see also Drinkwater et al. 2003). The absence of extended light as faint as

$27-28$ R mag arcsec^{-2} around seven of the Virgo UCDs also rules out the possibility that they are nuclei residing in extremely low surface brightness disks of spiral galaxies.

The available evidence indicates that the bright UCDs are unlikely to be the high-luminosity tail of the globular cluster system of NGC1399 (a possibility suggested by Drinkwater et al. 2000a and Mieske, Hilker & Infante 2002). The bright UCDs in Fornax and Virgo have absolute magnitudes ($M_B = -10.4$ to -13.1) that are brighter than the most luminous globular cluster in the Galaxy (ω Centauri, which has $M_B = -9.5$ mag) and in M31 (G1, with $M_B = -10.3$ mag). Many authors, however, have argued that both ω Cen and G1 might themselves be the remnant nuclei of tidally disrupted dE,N galaxies (e.g. Meylan et al. 2001; Bekki & Freeman 2003; Tsuchiya, Korchagin & Dinescu 2004; Bekki & Chiba 2004). The size–velocity dispersion properties of the Fornax UCDs are different to the relations for globular clusters (Drinkwater et al. 2003; Haşegan et al. 2005).

The Fornax results show that bright UCDs are spatially concentrated on the core of the cluster, with the core being defined here as the bright elliptical galaxy NGC1399. The UCDs, however, are less centrally concentrated than the globular cluster system of NGC1399 (Drinkwater et al. 2000a), but the difference is more modest when the globular cluster distribution of Dirsch et al. (2003) is used in preference to earlier data. The radial distribution of Virgo UCDs around M87 (Section 2.7) is much more extended than that of the M87 globular cluster system revealed in published studies, but an accurate comparison is difficult because the available data on the globular clusters are restricted to the immediate vicinity of M87. There is no convincing evidence (Section 2.8) that the mean radial velocity of the Virgo UCDs, or their velocity dispersion, is different to that of M87 or the M87 globular cluster system. Such a result which if found would indicate that the UCDs are not simply a more luminous component of the M87 globular cluster system, but a free-floating system in the core of the Virgo Cluster. Bekki et al. (2003) showed that dE,N galaxies are more likely to be tidally stripped if their orbits within the cluster have high eccentricities, a process that would produce a system of UCDs with a larger velocity dispersion than the system of dE,Ns under the tidal threshing model. The velocity dispersion of the 9 UCDs, however, is slightly smaller than that of dE,N galaxies in the same area satisfying the same velocity selection criteria, although the two values are statistically consistent.

Fornax UCD 3 consists of a bright, highly compact core within a more extended envelope. It is difficult to explain such an object as being an unusually luminous globular cluster, whereas objects of this kind are explicitly predicted by the tidal threshing model (Bekki et al. 2003). The tidal threshing model also predicts that some UCDs may be accompanied by discrete fainter companion objects, the result of tidal debris or globular clusters from the progenitor galaxy. One of the Virgo objects, UCD 6, has three objects lying nearby, as discussed in Sections 2.5 and 2.9. The nearby images might be expected to have colours similar to the UCD in the threshing model were they physically associated. The result from Section 2.5 that the colours are different suggests that they may be background galaxies/foreground stars.

Haşegan et al. (2005) performed a careful study of objects in the immediate vicinity of M87 to investigate the connection between UCDs and the most luminous M87 globular clusters. Of the six objects around M87 for which they had high-resolution spectroscopy and HST imaging, two had properties indicating that they are likely to by very luminous globular clusters. The other four – on the basis of their sizes, velocity dispersions, colours and mass-to-light ratios – had properties more consistent with UCDs. Significantly, the mass-to-light ratios are higher than can be expected on the basis of normal stellar populations alone, indicating the likely presence of dark matter. In contrast, Drinkwater et al. (2003) found mass-to-light ratios for Fornax UCDs that, although high, did not unambiguously indicate the presence of dark matter. Haşegan et al. noted that one of their four M87 UCDs has properties consistent with the Fellhauer & Kroupa (2002) model for producing UCDs from star clusters formed in galaxy interactions.

Haşegan et al. (2005) also identified candidate UCDs from HST Advanced Camera for Surveys imaging (Côté et al. 2004), using either published velocity data or surface brightness fluctuations to assess the likelihood that they lie in the Virgo

Cluster. Some of these show evidence of small haloes, like Fornax UCD3 of Drinkwater et al. (2000a; see also Hilker et al. 1999, Phillipps et al. 2001), but in contrast to the nine objects described in Section 2. Such compact haloes are explicitly predicted by the tidal threshing model of Bekki, Couch, & Drinkwater (2001).

De Propris et al. (2005) found that the nuclei of a sample of 18 Virgo Cluster dE,N galaxies drawn from HST archive observations are generally smaller than the 5 Fornax UCDs of Drinkwater et al. (2000a). This could be interpreted as evidence against the tidal threshing model. However, a direct comparison between the two types of object is not straightforward because the five UCDs have absolute magnitudes that are generally brighter than the dE,N nuclei, having been identified in a survey of targets selected by apparent magnitude. Further observations of the most luminous dE,N nuclei will be necessary to clarify the connection between the brightest UCDs and nuclei.

The results presented here, including the comparison between the observed and predicted radial distributions within the Fornax Cluster, are broadly consistent with the predictions of the tidal threshing model (Bekki et al. 2001; Bekki et al. 2003) (Section 3.4). However, the Bekki et al. (2003) predicted UCD radial distribution around M87 extends as far as $2\overset{\circ}{.}5$, whereas the 2dF observations here extend only $1\overset{\circ}{.}0$ from M87: a direct comparison between the observed and predicted UCDs distributions is not possible in the Virgo Cluster.

The Virgo compact elliptical galaxy NGC4486B, one of the few galaxies with properties comparable to M32, lies in the region of M87, between M87 and Virgo UCD1 in Figure 3. Tidal stripping of its outer regions by M87 has been advocated as the cause of NGC4486B's unusual morphology (e.g. Faber 1973). The distribution of the UCDs does not appear to be symmetric about M87: 8 of the 9 are found northeast of a line running southeast–northwest through M87 (which corresponds approximately to the major axis of M87).

The new discoveries of fainter compact objects in the Fornax Cluster by Mieske, Hilker & Infante (2004) and Drinkwater et al. (2004, and in preparation) suggest that the bright UCDs (described in this paper, and by Hilker et al. 1999, Drinkwater et al. 2000a and Phillipps et al. 2001) may be only the bright tail of a population of compact objects in cluster cores. The luminosity function of the nuclei of dE,N galaxies (Lotz et al. 2001) spans the luminosities of the bright UCDs and extends to lower luminosities. The tidal threshing model therefore predicts a population of fainter compact objects in the cores of galaxy clusters. Bekki et al. (2003) predict 14 UCDs of all magnitudes in Fornax and 46 in Virgo. The predicted number in Fornax is significantly smaller than the numbers of faint compact objects of Mieske, Hilker & Infante (2004) and Drinkwater et al. (in preparation). The actual numbers of compact objects in the cluster cores expected from the tidal threshing model will be larger than the numbers of naked nuclei themselves because of the presence of globular clusters released from tidally disrupted galaxies (although these free globular clusters will have significantly lower luminosities than the naked nuclei), including tidally disrupted luminous galaxies as well as dwarfs (see Bassino et al. 2003 for a discussion of intracluster globular clusters). The discovery of these objects in the nearest galaxy clusters is complemented by the identification of candidate UCDs in the Abell 1689 cluster (at a redshift $z = 0.18$) from imaging data by Mieske et al. (2004).

Mieske, Hilker & Infante (2004) compared the colors of Fornax UCDs with globular clusters and dE,N nuclei. The bright UCDs had $(\mathrm{V–I})_J$ colors that were slightly redder by 0.1 mag than the nuclei of dE,N galaxies. The tidal threshing hypothesis would predict that the nuclei and UCDs would have similar colors if star formation in the nuclei in dE,Ns had ceased before the disruption processes which produced the UCDs had begun. Had star formation continued in the nuclei of the surviving dE,Ns after tidal threshing had begun in those galaxies destined to become UCDs, the surviving dE,Ns could have bluer colors than the UCDs today. The observation that UCDs are redder than dE,N nuclei could therefore be interpreted as evidence that tidal threshing curtailed star formation in dE,N nuclei before nucleus star formation was complete.

Fellhauer & Kroupa (2002) argued that UCDs might be the result of mergers between massive star clusters formed in galaxy interactions. These merged objects will age following the end of their star formation to produce compact objects with

early-type galaxy spectra and half-light radii $\simeq 40$ to 160 pc. These are comparable to, or larger than, the observed sizes of the first five Fornax bright UCDs determined with the HST (Drinkwater et al. 2003). Maraston et al. (2004) measured the velocity dispersion of the stellar population in the giant star cluster W3 in the merged galaxy NGC7252, finding a value of 45 ± 5 km s^{-1}. This is larger by factors ranging from 1.2 to 1.9 than the first five Fornax UCDs (Drinkwater et al. 2003). W3 is likely to evolve over time into an object similar to the bright UCDs. Massive star clusters can therefore explain many of the observed properties of UCDs. Fellhauer & Kroupa (2005) modelled the formation of W3 by the merging of star clusters formed in the galaxy interaction which produced NGC7252. They predict that W3 has a compact core surrounded by a more extended halo; this has similarities to Fornax UCD3, which has a halo with an exponential scale length of 60 pc. UCDs with such envelopes are also directly predicted by the tidal threshing model.

Further observations in the Virgo Cluster will be needed to establish the distance from M87 at which the UCD radial distribution falls off, which would be an important test of the models for the origin of the UCDs. Bekki et al. (2003) predicted a cutoff at 2.°5 (700 kpc) from M87 in the tidal threshing model, significantly beyond the limits of the current survey (which currently reaches 1°, with poorer sampling beyond 0.°6 from M87).

5. Conclusions

New 2dF observations of star-like objects in a 1.°0 radius region centered on M87 in the Virgo Cluster have found 9 objects with properties similar to the bright Fornax UCDs. The discovery of UCD galaxies in the Virgo Cluster shows that this recently recognized class of objects is not peculiar to Fornax, and implies that UCDs are a common phenomenon in all galaxy clusters. These objects have sizes $\ll 100$ pc and blue absolute magnitudes $M_B = -10$ to -13; they are not clearly resolved by ground-based CCD imaging and do not have extended low surface brightness halos. If they can be found in sufficient numbers, the UCDs would be important test particles riding in the cluster gravitational potential.

We describe the properties of a sixth bright UCD in the Fornax Cluster using data from the 2dF Fornax Cluster Spectroscopic Survey. It is unresolved in available Schmidt photographic imaging data, has a blue photographic magnitude of $b_j = 19.4$ (equivalent to a blue absolute magnitude of $M_B = -12.0$), and has an early-type galaxy spectrum. It is more luminous than most of the objects in the recently discovered fainter compact-object population of Mieske, Hilker & Infante (2004) and Drinkwater et al. (in preparation). With new data from two additional fields, the Fornax 2dF observations extend to 3° (equivalent to a projected distance of 1.0 Mpc) from NGC1399, the bright elliptical galaxy at the core of the cluster. The observations have established that within the Fornax Cluster, bright UCDs lie exclusively within 0.°5 of NGC1399. The cutoff in their radial distribution (a projected distance of 170 kpc from NGC1399) is very close to that predicted by Bekki et al. (2001) in the tidal threshing model in which the UCDs are the remnant nuclei of galaxies that suffered tidal disruption due to repeated passes of a massive galaxy (NGC1399 in the case of the Fornax Cluster). Their distribution is slightly broader than that of the NGC1399 globular cluster system.

The available evidence is consistent with the UCDs being the remnant nuclei liberated via tidal threshing of dE,N galaxies. Many of the observed properties are also consistent with models of luminous star clusters formed in galaxy interactions. Seen in this light, characterizing the properties of the UCD population in a galaxy cluster is a potential gauge of the long-term effects of tidally-induced evolution over the lifetime of a galaxy cluster.

Acknowledgements

These observations were made using the 2dF spectrograph at the Anglo-Australian Observatory. We wish to thank the support and encouragement given by the AAO staff. This work made use of data from the United Kingdom Schmidt Telescope scanned by the APM Machine. Other imaging data were recorded with the Isaac Newton Telescope of the Isaac Newton Group in La Palma and provided by the ING Archive at the U.K. Astronomy Data Centre, Cambridge. Other photographic data from the United Kingdom Schmidt

Telescope were scanned by the SuperCOSMOS plate machine at the Royal Observatory Edinburgh. The stack of 63 UKST films was produced by the SuperCOSMOS Unit at the Royal Observatory Edinburgh.

Part of the work reported here was done at the Institute of Geophysics and Planetary Physics, under the auspices of the U.S. Department of Energy by Lawrence Livermore National Laboratory under contract No. W-7405-Eng-48 and has also been supported by the National Science Foundation under grant No. 0407445.

We thank the anonymous referee for detailed comments that have improved the paper.

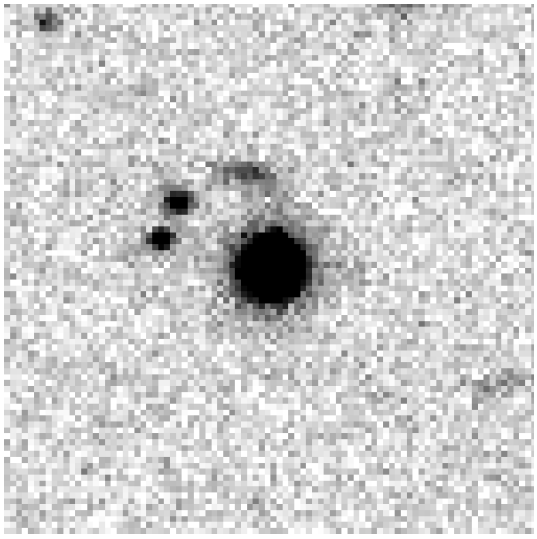

Fig. 12.— A CCD image of Virgo UCD 6. A 30″ × 30″ region around UCD 6 is shown based on a 25 min B-band integration with the Isaac Newton Telescope in 1.″1 seeing.

REFERENCES

Bailey, J., Glazebrook, K., Bridges T. 2000, *2dF Users' Manual*, Anglo-Australian Observatory

Bassino, L. P., Cellone, S. A., Forte, J. C., Dirsch, B., A&A, 399, 489

Bassino, L. P., Muzzio, J. C., Rabolli, M. 1994, ApJ, 431, 634

Bekki, K., Chiba, M. 2004, A&A, 417, 437

Bekki, K., Couch, W. J., Drinkwater, M. J. 2001, ApJ, 522, L105

Bekki, K., Couch, W. J., Drinkwater, M. J., Shioya, Y. 2003, MNRAS, 344, 399

Bekki, K., Freeman, K. C. 2003, MNRAS, 346, L11

Bessell, M. S., 1979, PASP, 91, 589

Binggeli, B., Cameron, L. M. 1993, A&A, 98, 297

Binggeli, B., Sandage, A. R., Tammann, G. A. 1985, AJ, 90, 1681

Blanchard, A., Valls-Gabaud, D., Mamon, G. A. 1992, A&A, 264, 365

Cairós, L. M., Vílchez, J. M., González-Pérez, J. N., Iglesias-Páramo, J., Caon, N. 2001, ApJS, 133, 321

Corbin, M.R., Vacca, W. D. 2002, ApJ, 581, 1039

Côté, P., Blakeslee, J. P., Ferrarese, L., Jordán, A., Mei, S., Merritt, D., Milosavljevič, M., Peng, E. W., Tonry, J. L., West, M. J., 2004, ApJS, 153, 223

Deady, J. H., Boyce, P. J., Phillipps, S., Drinkwater, M. J., Karick, A., Jones, J. B., Gregg, M. D., Smith, R. M. 2002, MNRAS, 336, 851

De Propris, R., Phillipps, S., Drinkwater, M. J., Gregg, M. D., Jones, J. B., Evstigneeva, E., Bekki, K. 2005, SpJ, 623, L105

Dirsch, B., Richtler, T., Geisler, D.,Forte, J. C., Bassino, L. P., Gieren, W. P. 2003, AJ, 125, 1908

Doublier, V., Caulet, A., Comte, G. 1999, A&AS, 138, 213

Doublier, V., Kunth, D., Courbin, F., Magain, P. 2000, A&A, 353, 887, 2000

Drinkwater, M. J., Bekki, K., Couch, W. J., Phillipps, S., Jones, J. B., Gregg, M. D. 2002, in I.A.U. Symposium 207: Extragalactic Star Clusters, eds. D. Geisler, E. K. Grebel & D. Minniti, p. 287, astro-ph/0106375

Drinkwater, M. J., Gregg, M. D., Colless, M. M. 2001, ApJ, 548, L139

Drinkwater, M. J., Gregg, M. D., Couch, W. J., Ferguson, H. C., Hilker, M., Jones, J. B., Karick, A., Phillipps, S. 2004, PASA, 21, 375

Drinkwater, M. J., Jones, J. B., Gregg, M. D., Phillipps, S. 2000a, PASA, 17, 227

Drinkwater, M. J., Phillipps, S., Jones, J. B., Gregg, M. D., Deady, J. H., Davies, J. I., Parker, Q. A., Sadler, E. M., Smith, R. M. 2000b, A&A, 355, 915

Drinkwater, M. J., Gregg, M. D., Hilker, M. J., Bekki, K., Couch, W. J., Ferguson, H. C., Jones, J. B., Phillipps, S. 2003, Nat, 423, 519

Durrell, P. 1997, AJ, 113, 531

Faber, S. M., 1973 ApJ, 179, 423

Fellhauer, M., Kroupa, P. 2002, MNRAS, 330, 642

Fellhauer, M., Kroupa, P. 2005, MNRAS, 359, 223

Ferrarese, L. 2000, ApJ, 529, 745

Ferguson, H. C. 1989, AJ, 98, 367

Ferguson, H. C., Sandage, A. R. 1988, AJ, 96, 1520

Gil de Paz, A., Madore, B. F., Pevunova, O. 2003, ApJS, 147, 29

Gregg, M. D., Drinkwater, M. J., Hilker, M. J., Phillipps, S., Jones, J. B., Ferguson, H. C. 2003, Ap&SpSc, 285, 113

Hanes D. A., Côté, P., Bridges, T. J., McLaughlin, D. E., Geisler, D., Harris, G. L. H., Hesser, J. E., Lee, M. G. 2001, ApJ, 559, 812

Haşegan, M., Jordán, A., Côté, P., Djorgovski, S. G., McLaughlin, D. E., Blakeslee, J. P., Mei, S., West, M. J., Peng, E. W., Ferrarese, L., Milosavljević, M., Tonry, J. L., Merritt, D. 2005, ApJ, in press, astro-ph/0503566

Hilker, M., Infante, L., Viera, G., Kissler-Patig, M., Richler, T. 1999, A&AS, 134, 75

Irwin, M. J., Maddox, S. J., McMahon, R. 1994, Spectrum, 2, 14

Karick, A. M., Drinkwater, M. J., Gregg, M. D. 2003, MNRAS, 344, 188

Kazantzidis, S., Moore, B., Mayer, L. 2003, in *Satellites and Tidal Streams*, eds. F. Prada, D. Martínez-Delgado & T. Mahoney, publ. Astronomical Society of the Pacific, astro-ph/0307362

Kunth, D., Maurogordato, S., Vigroux, L. 1988, A&A, 204, 10

Kurtz, M. J., Mink, D. J. 1998, PASP, 110, 934

Lotz, J. M., Telford, R., Ferguson, H. C., Miller, B. W., Stiavelli, M., Mack, J. 2001, ApJ, 552, 572

Maddox, S. J., Sutherland, W. J., Efstathiou, G., Loveday, J. 1990a, MNRAS, 243, 692

Maddox, S. J., Efstathiou, G., Sutherland, W. J. 1990b, MNRAS, 246, 433

Maraston, C., Bastian, N., Saglia, R. P., Kissler-Patig, M., Schweizer, F., Goudfrooij, P., 2004, A&A, 416, 467

Meylan, G., Sarajedini, A., Jablonka, P., Djorgovski, S. G., Bridges, T., Rich, R. M. 2001, AJ, 122, 830

McLaughlin, D. E., Harris, W. E., Hanes, D. A. 1994, ApJ, 422, 486

Mieske, S., Hilker, M. J., Infante, L. 2002, A&A, 383, 823

Mieske, S., Hilker, M. J., Infante, L. 2004, A&A, 418, 445

Mieske, S., Infante, L., Benítez, N., Coe, D., Blakeslee, J. P., Zekser, K., et al. 2004, AJ, 128, 1529

Moore, B. 2003, in *Clusters of Galaxies: Probes of Cosmological Structure and Galaxy Evolution*, eds. J. S. Mulchaey, A. Dressler & A. Oemler, Carnegie Observatories Astrophysics Series, Volume 3, Cambridge University Press, astro-ph/0306596

Navarro, J. F., Frenk, C. S., White, S. D. M. 1996, ApJ, 462, 563

Nieto, J.-L., Prugniel, P. 1987, A&A, 186, 30

Parker, Q. A., Malin, D. 1999, P.A.S. Australia, 16, 288

Phillipps S. 1997, in *Wide-field Spectroscopy*, eds. E. Kontizas, M. Kontizas, D. H. Morgan & G. P. Vettolan publ. Kluwer Academic Publishers, Dordrecht, p. 281

Phillipps, S., Drinkwater, M. J., Gregg, M. D., Jones, J. B. 2001, ApJ, 560, 201

Phillipps, S., Parker, Q. A., Schwartzenberg, J. M., Jones, J. B. 1998, ApJ, 493, L59

Richtler, T., Dirsch, B., Gebhard, K., Geisler, D., Hilker, M., Alonso, M. V., Forte, J. C., Grebel, E. K., Infante, L., Larsen, S., Minniti, D., Rejkuba, M. 2004, AJ, 127, 2094

Schwartzenberg, J. M., Phillipps, S., Parker, Q. A. 1995, A&A, 293, 332

Strom, S. E., Forte, J. C., Harris, W. E., Strom, K. E., Wells, D. C., Smith, M. G. 1981, ApJ, 245, 416

Tsuchiya, T., Korchagin, V. I., Dinescu, D. I. 2004, MNRAS, 350, 1141

Tegmark, M., Silk, J., Rees, M. J., Blanchard, A., Abel, T., Palla, F. 1997, ApJ, 474, 1

Tonry, J.L., Davis, M. 1979, AJ, 84, 1511

Trentham, N., Hodgkin, S. 2002, MNRAS, 333, 423

This 2-column preprint was prepared with the AAS LaTeX macros v5.2.